JACS
JOURNAL OF THE AMERICAN CHEMICAL SOCIETY
Article
pubs.acs.org/JACS

Controlling the Degree of Polymerization, Bond Lengths, and Bond Angles of Plasmonic Polymers

Ariella Lukach,[†] Kun Liu,[†] Heloise Therien-Aubin,[†] and Eugenia Kumacheva*[,†,‡,§]

[†]Department of Chemistry, University of Toronto, 80 Saint George Street, Toronto, Ontario M5S 3H6, Canada

[‡]Department of Chemical Engineering and Applied Chemistry, University of Toronto, 200 College Street, Toronto, Ontario M5S 3E5, Canada

[§]The Institute of Biomaterials and Biomedical Engineering, University of Toronto, 4 Taddle Creek Road, Toronto, Ontario M5S 3G9, Canada

Supporting Information

ABSTRACT: Plasmonic polymers present an interesting concept that builds on the analogy between molecular polymers and linear chains of strongly interacting metal nanoparticles. Ensemble-averaged optical properties of plasmonic polymers are strongly influenced by their structure. In the present work, we formed plasmonic polymers by using solution-based assembly of gold nanorods (NRs) end-tethered with photoactive macromolecular tethers. By using postassembly ligand photo-cross-linking, we established a method to arrest NR polymer growth after a particular self-assembly time, and in this manner, using kinetics of step-growth polymerization, we achieved control over the average degree of polymerization of plasmonic polymers. Photo-cross-linking of ligands also enabled control over the internanorod distance and resulted in the increased rigidity of NR chains. These results, along with a higher structural integrity of NR chains, can be utilized in plasmonic nanostructure engineering and facilitate advanced applications of plasmonic polymers in sensing and optoelectronics.

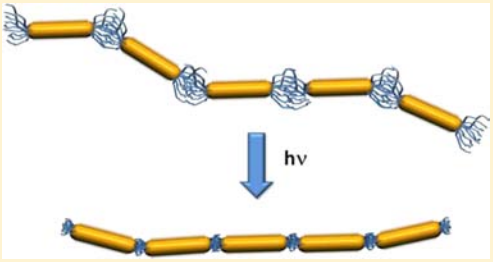

INTRODUCTION

Linear chains of metal nanoparticles (NPs) offer a captivating concept of plasmonic polymers, in which the NPs act as repeat units.[1] In the chains, interactions between surface plasmon resonances of NPs lead to the dependence of optical properties of plasmonic polymers on their structural characteristics, namely, their aggregation number, mutual NP orientation, and inter-NP spacing.[2] These properties correlate with the degree of polymerization, bond angles, and bond lengths, respectively, of the molecular analogues of plasmonic polymers. Because of the rich parameter space in tuning the structure of plasmonic polymers, their electric and magnetic responses can be engineered over a broad range, thereby offering routes to potential applications in optical nanocircuits,[3] nanoscale light transport (i.e., waveguides),[4] nanoantennae,[5] and sensing.[6]

Generally, plasmonic nanostructures with well-defined arrangements of NPs, for example, with controlled mutual alignments and interparticle distances, are fabricated on planar substrates by electron-beam lithography or focused ion-beam milling.[7] The self-assembly of metal NPs offers a cost-efficient alternative to top-down approaches by producing plasmonic nanostructures with a variety of geometries and reduced inter-NP distances, and combining NP building blocks with different sizes, shapes, and compositions.[8] In particular, the self-organization of inorganic NPs in polymer-like structures can be achieved by utilizing directional physical bonding between complementary or self-complementary ligands capping NP surface, in a manner resembling supramolecular polymerization.[9,10] Reversible noncovalent NP association can be realized by hydrogen bonding,[11−13] metal coordination,[14] hydrophobic forces,[15,16] and electrostatic interactions.[17] Because of the reversibility of NP self-assembly, their chains can be broken and recombined under the action of external stimuli such as pH or temperature.[18−20]

While supramolecular polymerization of metal NPs is an appealing strategy, it has several limitations. For example, although for a particular self-assembly time, the average degree of polymerization of plasmonic polymers can be conveniently predicted by the kinetics of step-growth polymerization,[21] continuous growth of NP chains precludes control over their optical properties. The self-assembly of NPs can be stopped by encapsulating NP ensembles within a polyelectrolyte shell[22] or by "competitive binding of ligands" preventing NP association.[23] These approaches are promising for practical applications of NP chains; however, encapsulation may screen the polymer nature of the chains, and more importantly their optical properties. This can impede their use in many applications, for example, refractive index sensors[24] and surface-enhanced Raman scattering (SERS)-based sensors.[25] The method utilizing competitive binding of ligands involves a complicated surface chemistry, which heavily relies on stoichiometry and leads to a small population of chains with desired lengths and morphologies.

Received: September 24, 2012
Published: October 18, 2012

dx.doi.org/10.1021/ja309475e | J. Am. Chem. Soc. 2012, 134, 18853−18859

Second, attaining small spacing between adjacent NPs is a crucial requirement for realizing collective optical properties of plasmonic polymers.[26] This constraint limits the use of macromolecular ligands, while oligomer ligands with relatively low molecular weights show a weaker propensity for association.[16] Finally, solution-based NP self-assembly of plasmonic polymers generally yields flexible chains, especially when macromolecular ligands are used. It is desirable to achieve at least partial control of chain rigidity, as it affects the formation of secondary polymer structures, for example, rings,[14] and the intensity of SERS.[27] Chain rigidity was increased by assembling gold nanorods (NRs) in the end-to-end manner by using rigid aromatic dithiol linkers.[28] This approach relied on covalent bonding between adjacent NRs and required specific surface chemistry and stoichiometry between the bifunctional ligands and the NRs.

Here, we report a new strategy for controlling the structural characteristics of plasmonic polymers formed by gold NRs end-terminated with poly(styrene-*co*-isoprene) ligands. Solution-based NR assembly was triggered by reducing the quality of solvent for the poly(styrene-*co*-isoprene) end-tethers, which reduced their exposure to the solvent by forming physical bonds between the NR ends. After a particular assembly time, the ligands were photo-cross-linked, which resulted in several important effects: a suppressed bond-forming ability of the poly(styrene-*co*-isoprene) ligands, a substantial reduction in the internanoparticle distance, and a notable increase in angles between adjacent NRs. These effects were tuned by varying the time of irradiation, that is, the extent of cross-linking.

The proposed strategy offers the following useful features in the design and construction of plasmonic polymers:

(i) the ability to control their average degree of polymerization (the average aggregation number) by tuning the time of self-assembly and/or the time of photo-irradiation;
(ii) the capability to control internanoparticle distances;
(iii) the enhanced colinearity of the NRs (important for SERS applications);
(iv) the capability of "freezing" of NR assemblies in solution for subsequent characterization and handling.

EXPERIMENTAL SECTION

Materials. Hexadecyltrimethylammonium bromide (CTAB, 99%), sodium borohydride ($NaBH_4$, 98%), hydrogen tetrachloroaurate (III), a 30% solution in dilute hydrochloric acid, and L-ascorbic acid were purchased from Sigma-Aldrich (Canada). Dimethylformamide (DMF) and tetrahydrofuran (THF) were purchased from Fisher Scientific and used as received. Azo-bis(isobutyronitrile) (AIBN, 99%, Aldrich) was recrystallized from methanol. Deionized water (Millipore Milli-Q grade) with resistivity of 18.2 MΩ was used in all of the experiments.

Synthesis of Thiol-Terminated Random Poly(styrene-*co*-isoprene) (PS-*co*-PI) Copolymer. The copolymer was synthesized by living anionic copolymerization of styrene and isoprene monomers. Polymerization was initiated with *n*-butyllithium (*n*-C_4H_9Li) in toluene/diglyme mixture at 20 °C, and terminated by injection of ethylene sulfide. The random copolymer SH-PS_{104}-*co*-PI_{18} consisted of approximately 63% of 3,4 isoprene units, as characterized by GPC and NMR. The copolymer had the number average molecular weight M_n = 12 000 g mol^{-1} and a polydispersity of 1.08.

Synthesis of Gold NRs and Ligand Exchange. Gold NRs stabilized with CTAB were prepared using a modified protocol of the "seed-mediated" approach developed by Nikkobakht and El-Sayed (see Supporting Information).[29] The average length and diameter of the NRs were 40 and 9 nm, respectively. After synthesis, CTAB on the NR ends was replaced with the PS-*co*-PI copolymer following a previously reported procedure.[15] Approximately 0.05 mL of the concentrated solution of NRs was rapidly injected into 1 mL of 0.02 wt % solution of PS-*co*-PI in tetrahydrofuran (THF) under sonication. The mixture was maintained at ambient conditions overnight. The free PS-*co*-PI copolymer was separated from the NR solution by 10 centrifugation cycles, which were 30 min long, at 10 000 rpm, and the NRs were redispersed in THF.

End-to-End Self-Assembly of NRs. A stock solution (0.1 g) of modified NRs in THF was dried and redispersed in 0.235 g of dimethylformamide (DMF). A 0.015 g solution of azo-bis-isobutyronitrile (AIBN) in DMF (1 wt %) was added, and the solution was shaken for several seconds. The self-assembly of the NRs was triggered by dropwise addition of the DMF/water mixture at water concentration C_w = 30 wt % to achieve the total final concentration of water in the NR solution of C_w = 15 wt %. The self-assembly process was monitored by using spectroscopy (a Varian Cary 5000 UV−vis spectrometer), transmission electron microscopy (TEM), and scanning electron microscopy (SEM) (Hitachi H-7000 transmission electron microscope and Hitachi HD-2000 scanning transmission electron microscope). Images were analyzed using ImageJ and MATLAB programs.

Photo-Cross-Linking of PS-*co*-PI. After a particular self-assembly time, the solutions of NRs were placed under a UV-A lamp (Hönle, UVAPrint 40C, λ = 365 nm, I = 30 mW cm^{-2}, at a distance of 10 cm from the lamp), which was warmed before the experiments for 10 min to achieve steady power. The samples were irradiated for time intervals in the range from 0 to 25 min. Carbon spectra of the statistical copolymer before and after photo-cross-linking were recorded on an Agilent DD2 500 MHz spectrometer with an Agilent HC 5-mm XSens cryogenically cooled probe. A ^{13}C pulse width of 30° was used, acquiring a spectral window of 28 750 Hz (230 ppm) using 64k points. The ^{13}C 90° pulse width was 21.4 μs. All pulse sequences used were provided by Agilent.

Characterization of Bond Angles in NR Chains. Image analysis of TEM images (Figure S1a) was performed using a Matlab program. Each NR in a chain was approximated as an ellipsoid (Figure S1b). The angle between the long axes of two neighboring ellipsoids, θ_i, was measured as shown in Figure S3c, where the subscript "i" indicates the ith NR pair. Statistical analysis of the distribution of angle was realized using the nonparametric Mann−Whitney test (statistical p-value = 0.05).[30]

RESULTS

Figure 1 shows a schematic of a plasmonic polymer composed of gold NRs that are linked in the chain with macromolecular

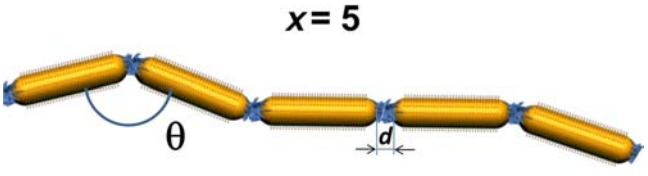

Figure 1. Illustration of the plasmonic polymer formed by gold NRs.

ligands. The number of NRs in the chain characterizes the degree of polymerization of the plasmonic polymer, x. The bond length is given by the shortest end-to-end distance, d, between the two neighboring NRs in the chain. The bond angle, θ, is defined as the angle between the long axes of the two neighboring NRs. We note that self-assembled plasmonic polymers are characterized by the average values of x, d, and θ.

The approach to NR self-assembly is schematically illustrated in Figure 2. Following NR synthesis and ligand exchange, CTAB ligands at the NR ends were replaced with poly(styrene-*co*-isoprene) (PS-*co*-PI) copolymer molecules (Figure 2a).[31]

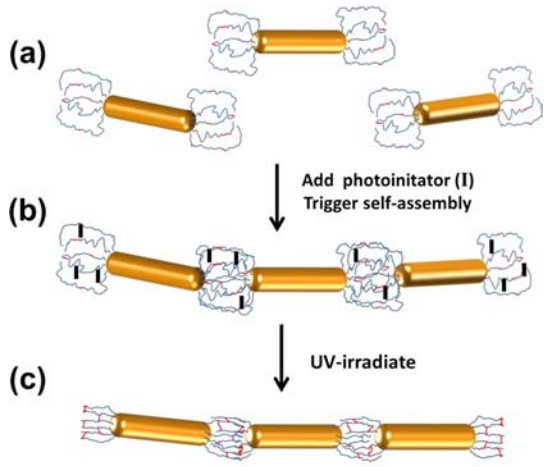

Figure 2. Schematic of photo-cross-linking of PS-*co*-PI ligands tethered to the ends of gold NRs. (a) Individual NRs in DMF solution. (b) Self-assembled NR chain containing a photoinitiator AIBN (denoted as **I**) partitioned in the PS-*co*-PI environment between the ends of the NRs chains and at the free ends of the NRs. (c) Photo-cross-linked NR chains.

The amphiphilic NRs were dispersed in DMF, a good solvent for the copolymer ligands. A hydrophobic photoinitiator, azo-bis-isobutyronitrile (AIBN), was added to the NR solution. Addition of water to the NR solution reduced the quality of solvent for PS-*co*-PI and AIBN molecules. To minimize unfavorable interactions with a poor solvent, the hydrophobic copolymer ligands capping NR ends formed physical bonds with the adjacent NRs, thereby organizing them in the end-to-end manner in a colloidal polymer. The hydrophobic AIBN molecules were partitioned in the copolymer "compartments" between the ends of neighboring NRs in the chain and at the free ends of the chain (Figure 2b), as well as on the individual NRs (not shown in the figure).

After a particular time of self-assembly, t_{SA}, the solution of NRs was irradiated with ultraviolet light at a wavelength 365 nm, causing AIBN decomposition into radicals.[32] We note that this irradiation wavelength, as well as the absorption peak of AIBN at ~350 nm (Supporting Information, Figure S2), did not overlap with the plasmonic resonances of gold NRs. Because upon photoirradiation, polymers with pendant double bonds can undergo intermolecular cycloaddition,[33−35] we hypothesized the reaction of the compartmentalized AIBN radicals with isoprene moieties in the copolymer ligands would lead to the permanent chemical cross-linking of the PS-*co*-PI copolymer. Using ^{13}C NMR spectroscopy of photoirradiated PS-*co*-PI copolymer in the DMF/water solution (C_w = 6 wt %), we confirmed the disappearance of the C=C bonds and the appearance of new aliphatic peaks (Supporting Information, Figure S3).[36,37]

We monitored the end-to-end self-assembly of the NRs by imaging NR chains (Figure S4) and by acquiring the absorbance spectra of the NR solution. Figure 3a shows the variation in absorbance spectra of the NRs following their self-assembly in chains before and after photoirradiation of the NR solution. The association of the NRs in chains after self-assembly time of t_{SA} = 7 h led to a 90 nm red-shift in their longitudinal plasmon resonance band (Figure 3), in agreement with earlier works.[2b,38,39] At this point, the solution was UV-irradiated for 25 min, and the system was subsequently equilibrated for 19 h. The longitudinal surface plasmon resonance band (λ_{LSPR}) exhibited a 60 nm red shift immediately after irradiation. Further incubation of the NR solution for 19 h did not change the spectral position of the LSPR (Figure 3a). To check the stability of the self-assembled structures after irradiation, the system was diluted with a large amount of DMF to reduce the total content of water to C_w = 2 wt %. At this concentration of water, the quality of the solvent is not sufficiently poor to cause NR assembly.[15] Thus, we expected the disintegration of NR chains, if photoirradiation would not lead to their permanent cross-linking. Upon dilution, the λ_{LSPR} exhibited a blue shift; however, it did not reach the spectral position of the original λ_{LSPR} of the individual NRs before the self-assembly (Figure 3a).

Figure 3a shows several important effects. First, attraction between the NRs end-tethered with PS-*co*-PI ligands led to the end-to-end NR association, resulting in the red shift of λ_{LSPR}. Second, after UV-irradiation, λ_{LSPR} exhibited an additional red shift. This effect could originate from the continuing growth of NR chains, from the reduced distance between the NR ends (leading to a stronger plasmonic coupling between the NRs), or from both effects. While the possibility of further growth of NR chains will be discussed later, Figure 3b,c shows that the inter-NR distance reduced after photo-cross-linking of the PS-

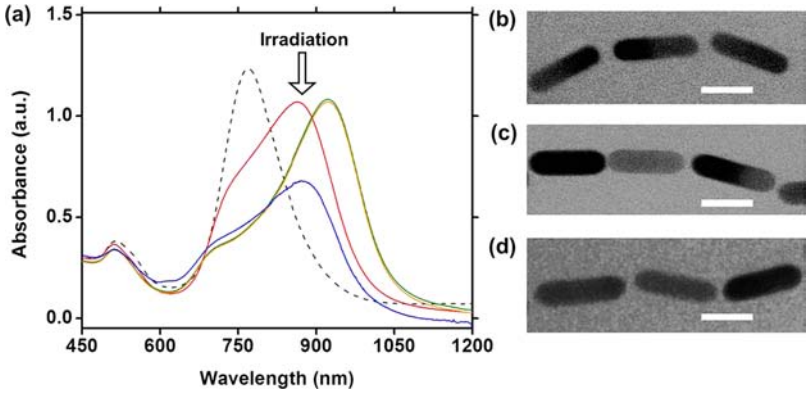

Figure 3. (a) Absorbance spectra of gold NRs undergoing self-assembly into linear chains before and after photoirradiation: individual NRs (dashed line), NR chains after 7 h-long self-assembly (red line), 10 min and 19 h after photoirradiation (green and orange lines, respectively), and after dilution of the system with DMF to C_w = 2 wt % (blue line). (b−d) TEM images of the fragments of NR chains before (b) and after (c) photo-cross-linking, and following dilution to C_w = 2 wt % (d). Scale bars are 25 nm.

dx.doi.org/10.1021/ja309475e | J. Am. Chem. Soc. 2012, 134, 18853−18859

co-PI ligands, due to the formation of a more compact network structure. Third, upon addition of a good solvent, blue shift of the λ_{LSPR} was observed. This effect originated from a weaker plasmonic coupling between the NRs, caused by a noticeable increase in the inter-NR distance due to the swelling of the copolymer network (Figure 3d).

To verify the role of photo-cross-linking of the copolymer ligands, we conducted a series of control experiments, in which we monitored the change in absorbance spectra of the NRs in the course of their self-assembly (i) without photoirradiation, (ii) in the absence of AIBN, and (iii) without photoirradiation and in the absence of AIBN (Table 1). We also examined the reversibility of the NR self-assembly by diluting the system with DMF (a good solvent for the copolymer ligands) to C_w = 2 wt %. None of the control systems showed the effects presented in Figure 3. Instead, in all of these experiments, we observed a continuous temporal red shift of λ_{LSPR} (suggesting NR assembly in the end-to-end manner), while dilution of the system with DMF led to the dissociation of the NR chains (Supporting Information, Figure S5). Thus, we conclude that photopolymerization was critically important for the termination of the self-assembly process.

Table 1. Control Experiments on the Self-Assembly and Dissociation of Plasmonic Polymers

system[a]	addition of AIBN	UV-irradiation	self-assembly	chain dissociation
S1	+	−	not terminated	+
S2	−	+	not terminated	+
S3	−	−	not terminated	+

[a]S1: NR self-assembly in the presence of AIBN without photoirradiation. S2: NR self-assembly in the absence of AIBN with photoirradiation. S3: NR self-assembly without photoirradiation in the absence of AIBN. The symbols "+" and "−" indicate that the event occurred or did not occur, respectively.

We examined the effect of the irradiation time, t_{ir}, of the solution of self-assembled NRs, on the bond length in the NR chains (Figure 1). For the irradiation time in the range $0 \le t_{ir} \le$ 25 min, with increasing t_{ir} the average distance between the neighboring NRs in the chains, d, noticeably reduced (Figure 4a−c). Quantitatively, this effect is presented in Figure 4d as the relative variation in d/d_0 versus t_{ir}, where d_0 is the average distance between the NR ends at t_{ir} = 0, respectively (d_0 = 5.3 nm). For irradiation time t_{ir} = 25 min, the value of d/d_0 was ∼55%, reaching ∼2.9 nm. We attribute the reduction in inter-NR distance to the cross-linking of the copolymer ligands.

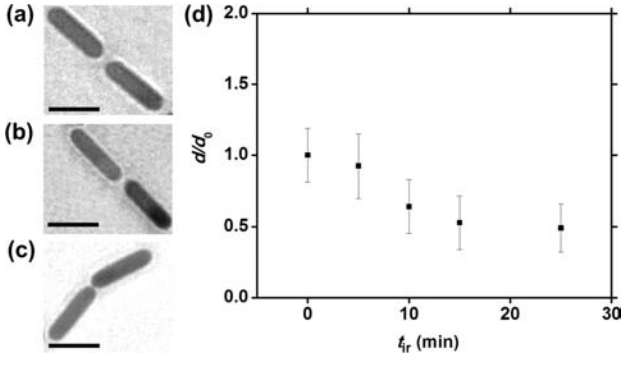

Figure 4. Representative TEM images of the pairs of adjacent NRs in the chains after irradiation for 0 (a), 10 (b), and 25 (c) min. Scale bars are 35 nm. (d) Effect of irradiation time on the relative reduction in the spacing between the neighboring NRs in the chain. The analysis is based on image analysis of 100 inter-NR gaps. d_0 = 5.3 nm.

Next, we examined the effect of the irradiation time, t_{ir}, on the growth of NR chains. After NR self-assembly time of 1.5 h, the solution was irradiated for the time in the range $0 \le t_{ir} \le 25$ min. The temporal variation in the average aggregation number of the chains was characterized by the monitoring the variation in absorbance spectra of the NRs. In addition, drawing on the analogy between step-growth polymerization and the self-assembly of plasmonic polymers, we determined the number average degree of polymerization, $\bar{X}_n$, of the NR chains. The value of $\bar{X}_n$ was determined as $\bar{X}_n = \sum n_x x / \sum n_x$, where x is the number of NRs in the chain and n_x is the number of chains containing x NRs.

Figure 5 shows the temporal variation in the shift of λ_{LSPR} during the course of self-assembly without and after photoirradiation, along with the initial and final values of $\bar{X}_n$. Photoirradiation of the solution for 25 min led to a stabilized λ_{LSPR} ($\Delta\lambda_{LSPR} \approx 0$), while for t_{ir} = 0 and t_{ir} = 5 min, the value of $\Delta\lambda_{LSPR}$ exhibited a continuous growth. A slower growth of $\Delta\lambda_{LSPR}$ in the system irradiated for 5 min, as compared to the control system (t_{ir} = 0), indicated a reduced ability of NRs to assemble in chains. We correlated the change in $\Delta\lambda_{LSPR}$ with the value $\bar{X}_n$ determined 24 h after photoirradiation. Starting from $\bar{X}_n$ = 2.25, the value $\bar{X}_n$ = 5.29 was achieved for the control system, while for t_{ir} = 5 min, the growth of polymers was suppressed to $\bar{X}_n$ = 2.80. For t_{ir} = 25 min, the value of $\bar{X}_n$ was invariant ($\bar{X}_n$ = 2.22). By using the analogy between NR self-assembly and step-growth polymerization,[21] we estimated conversion, p, of NRs into chains as $p = 1 - 1/\bar{X}_n$.[40] After 24 h, the value of p increased from 0.55 to 0.81 and 0.64 for the control system and the system irradiated for 5 min, respectively. Conversion in the system irradiated for 25 min remained invariant.

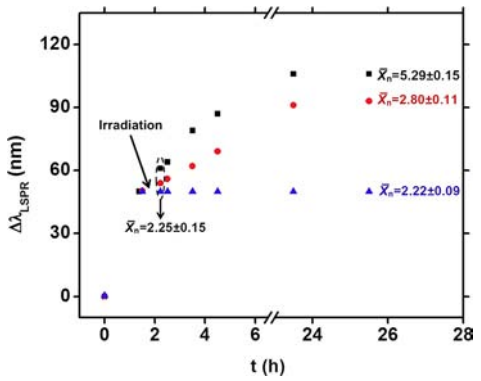

Figure 5. Effect of irradiation time on the shift in λ_{LSPR}. The initial and final values of the number average degree of polymerization, $\bar{X}_n$, for t_{ir}= 0, 5, and 25 min are shown with ■, red ●, and blue ▲, respectively. The values of $\bar{X}_n$ were measured 20 min and 24 h after irradiation.

Because the self-assembly of gold NRs resembles reaction-controlled step-growth polymerization, with $\bar{X}_n$ increasing linearly with time,[21] it can be expected that by terminating NR self-assembly by photoirradiation after a particular self-assembly time, t_{SA}, plasmonic polymers with a well-defined, permanent $\bar{X}_n$ can be produced. We carried self-assembly of the NRs for different time intervals, after which the system was subjected to photoirradiation for 25 min. Figure 6 shows the

dx.doi.org/10.1021/ja309475e | J. Am. Chem. Soc. 2012, 134, 18853−18859

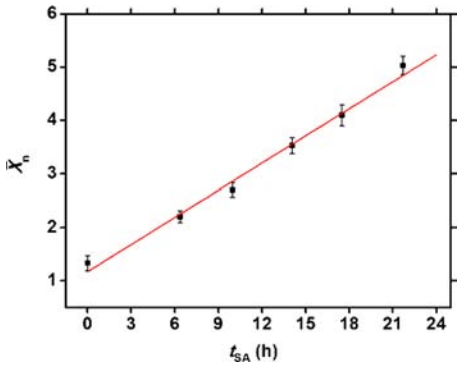

Figure 6. Variation in the average degree of polymerization, $\bar{X}_n$, of the NR chains photo-cross-linked after varying self-assembly time, t_{SA}. The line is shown for eye guidance.

variation in $\bar{X}_n$ of the cross-linked NR chains with the time of self-assembly. The variation in $\bar{X}_n$ versus t_{SA} followed a linear trend suggesting that photoirradiation did not affect the variation in $\bar{X}_n$ characteristic of step-growth polymerization. Following photoirradiation, the values of $\bar{X}_n$ remained invariant for 21 h.

Finally, we explored the effect of cross-linking of the PS-*co*-PI tethers on the rigidity of the NR chains. We examined the distribution of bond angles between two adjacent NRs (as shown in Figure 1) for two populations of NR chains, short chains with $\bar{X}_n \leq 5$ and long chains with $\bar{X}_n \geq 12$. For each population, we used noncross-linked NR chains with the corresponding values of $\bar{X}_n$ as a control system. Figure 7a shows that after cross-linking, short NR chains had a notably higher fraction of large ($\theta > 120°$) bond angles than did noncross-linked chains. While bond angles in the NR chains dried on the TEM grid may not reflect the real bond angles existing in solution, this result suggested a higher rigidity of cross-linked chains, which was caused by their reduced conformational entropy.[41] In contrast, no statistical difference in the distribution of bond angles was observed for cross-linked and noncross-linked NR long chains (Figure 7b). This effect was attributed to the dominant effect of stretching of the long chains on the TEM grid, caused by surface tension-driven flow, which was consistent with our earlier findings.[21]

DISCUSSION

Photo-cross-linking of PS-*co*-PI end-tethers at a particular stage of NR self-assembly resulted in several important effects that were not originally expected. A suppressed ability of PS-*co*-PI ligands to form physical bonds between the ends of NR was the first consequence of photo-cross-linking, which resulted in stopping polymer growth. This effect offered a new approach to arresting NP self-assembly after a particular time interval, without the need to encapsulate NP ensembles with polyelectrolytes or add multiple ligands.[21,22] Photoinduced deactivation of bonding-forming ligands originated from several effects. First, cross-linking suppressed interpenetration of copolymer ligands attached to the NR ends when the quality of the solvent was reduced.[42] Second, cross-linking of copolymer ligands led to up to ~40% reduction in the dimensions of the copolymer "pom-pom" at the NR end (Figure 4d). Both effects resulted in weaker hydrophobic interactions between the ligands at the NR ends.[43] Finally, upon cross-linking of the ligands, a polymer network with increased rigidity formed at the NR end, which counteracted its deformation to maximize attraction between self-assembling NRs.

The second effect of photo-cross-linking of the PS-*co*-PI ligands located between the ends of NRs in the chains was a controllable reduction (up to 55%) of the distance between the neighboring NRs. The ability to realize very small spacing between the NRs, still using macromolecular ligands for their assembly, has important implications for potential applications of NR ensembles, for example, as waveguides,[4] or in SERS-based sensing.[27,44] In principle, the distance between the NRs in the chains could be controlled by either the quality of solvent for the polymer tethers or the molecular weight of the polymer;[15,16] however, these variables influenced other properties of the NR chains, for example, the degree of polymerization[16] or the number of defects caused by NR side-by-side assembly.[45] Therefore, post self-assembly reduction in the distance between the NR ends offered a favorable method for reducing inter-NR distance.

Third, photo-cross-linking led to an increase in the rigidity of NR chains. While using TEM imaging, we observed a higher NR colinearity for short ($\bar{X}_n \leq 5$) NR chains; we believe that both short and long chains experienced a similar increase in bond angles. Because the colinearity of NRs in the chains influences their extinction and SERS properties, ligand cross-linking can serve as a facile method for the enhancement of this property.

Permanent cross-linking of self-assembled NR chains in solution enables their further manipulation, for example,

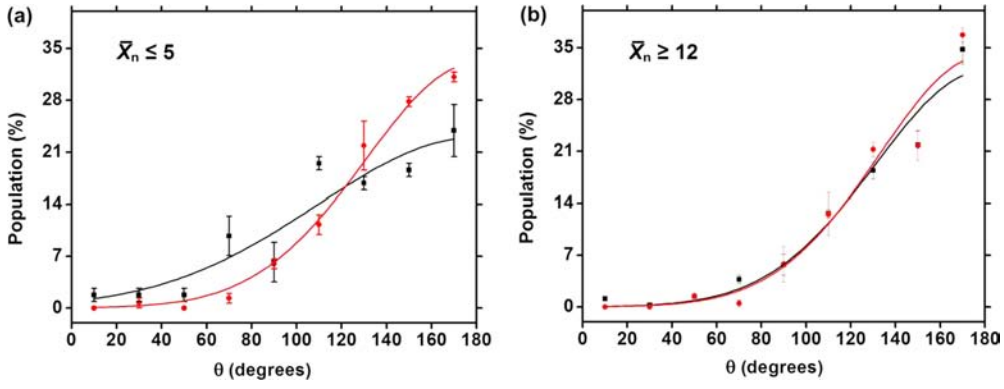

Figure 7. Variation in the distribution of bond angles, θ, for (a) short and (b) long chains before (black curve) and after (red curve) photoirradiation. Approximately 125 NR pairs were analyzed for each population of chains. The lines are shown for eye guidance.

dx.doi.org/10.1021/ja309475e | J. Am. Chem. Soc. 2012, 134, 18853−18859

alignment or transfer between different solvents or substrates, and allows their more reliable characterization by imaging techniques. It also offers, in principle, the capability to draw analogies between plasmonic polymers and their molecular counterparts by minimizing the effects of the substrate and solvent evaporation. We note that post self-assembly cross-linking of plasmonic polymers differs from the formation of NR chains using covalent linkers:[1g,27] the reversibility of self-assembly allows the formation of structures with high morphological integrity and a lower occurrence of defects.[45]

■ SUMMARY

We have developed a new strategy for controlling structural characteristics of plasmonic polymers formed by gold NRs. Postassembly photo-cross-linking of ligands attached to the NR ends stopped NR self-assembly, enabling control over the number average degree of polymerization of the NR chains (following the reaction kinetics of step-growth polymerization). By varying the time of photoirradiation of the system, we tuned the distance between the NRs in the chain. Moreover, we have shown that following ligand photo-cross-linking, the NRs in the chains became more linear. All of the above, along with increased structural stability of plasmonic polymers, can facilitate their advanced applications in sensing and optoelectronics.

■ ASSOCIATED CONTENT

Ⓢ Supporting Information

Synthesis of gold nanorods, ^{13}C NMR spectrum of poly(styrene-*co*-isoprene), low magnification TEM image of photo-cross-linked self-assembled NR chains, description of characterization of bond angles in NR chains using TEM imaging and MATLAB, absorbance spectra of control systems, and absorption spectrum of AIBN in DMF. This material is available free of charge via the Internet at http://pubs.acs.org.

■ AUTHOR INFORMATION

Corresponding Author

ekumache@chem.utoronto.ca

Notes

The authors declare no competing financial interest.

■ ACKNOWLEDGMENTS

We acknowledge Ilya Gourevich and Dr. Neil Coombs of the Center of Nanostructure Imaging for assistance in electron microscopy experiments. We thank Dr. Alla Petukhova and Dr. Valeriy Zaboristov for assistance in the synthesis of thiol-terminated poly(styrene-*co*-isoprene) copolymer. This work was funded by Biopsys (NSERC Canada Strategic Network for Bioplasmonic Systems). We also acknowledge the Canadian Foundation for Innovation (project number 19119), and the Ontario Research Fund for funding of the Centre for Spectroscopic Investigation of Complex Organic Molecules and Polymers. K.L. thanks the Ontario Ministry of Economic Development and Innovation for the Post-Doctoral Fellow award.

■ REFERENCES

(1) (a) Slaughter, L. S.; Willingham, B. A.; Chang, W.-S.; Chester, M. H.; Ogden, N.; Link, S. *Nano Lett.* **2012**, *12*, 3967−3972. (b) Gao, B.; Arya, G.; Tao, A. R. *Nat. Nanotechnol.* **2012**, *7*, 433−437. (c) Yang, M.; Chen, G.; Zhao, Y.; Silber, G.; Wang, Y.; Xing, S.; Han, Y.; Chen, H. *Phys. Chem. Chem. Phys.* **2010**, *12*, 11850−11860. (d) Wang, L.; Zhu, Y.; Xu, L.; Chen, W.; Kuang, H.; Liu, L.; Agarwal, A.; Xu, C.; Kotov, N. A. *Angew. Chem., Int. Ed.* **2010**, *49*, 5472−5475. (e) Nakata, K.; Hu, Y.; Uzun, O.; Bakr, O.; Stellacci, F. *Adv. Mater.* **2008**, *20*, 4294−4299. (f) Sardar, R.; Shumaker-Parry, J. S. *Nano Lett.* **2008**, *8*, 731−736. (g) Shibu Joseph, S. T.; Ipe, B. I.; Pramod, P.; Thomas, K. G. *J. Phys. Chem. B* **2006**, *110*, 150−157. (h) Lin, S.; Li, M.; Dujardin, E.; Girard, C.; Mann, S. *Adv. Mater.* **2005**, *17*, 2553−2559. (i) Murphy, C. J.; Sau, T. K.; Gole, A.; Orendorff, C. J. *MRS Bull.* **2005**, *30*, 349−355. (j) Caswell, K. K.; Wilson, J. N.; Bunz, U. H. F.; Murphy, C. J. *J. Am. Chem. Soc.* **2003**, *125*, 13914−13915.

(2) (a) Zhu, Z.; Liu, W.; Li, Z.; Han, B.; Zhou, Y.; Gao, Y.; Tang, Z. *ACS Nano* **2012**, *6*, 2326−2332. (b) Halas, N. J.; Lal, S.; Chang, W.-S.; Link, S.; Nordlander, P. *Chem. Rev.* **2011**, *111*, 3913−3961. (c) Barrow, S. J.; Funston, A. M.; Gómez, D. E.; Davis, T. J.; Mulvaney, P. *Nano Lett.* **2011**, *11*, 4180−4187. (d) Girard, C.; Dujardin, E.; Baffou, G.; Quidant, R. *New J. Phys.* **2008**, *10*, 105016. (e) Zhao, L.; Kelly, K. L.; Schatz, G. C. *J. Phys. Chem. B* **2003**, *107*, 7343−7350. (f) Maier, S. A.; Brongersma, M. L.; Kik, P. G.; Atwater, H. A. *Phys. Rev. B* **2002**, *65*, 193408. (g) Maier, S. A.; Kik, P. G.; Atwater, H. A. *Appl. Phys. Lett.* **2002**, *81*, 1714−1716.

(3) Engheta, N. *Science* **2007**, *317*, 1698−1702.

(4) (a) Liu, N.; Mukherjee, S.; Bao, K.; Li, Y.; Brown, L. V.; Nordlander, P.; Halas, N. J. *ACS Nano* **2012**. (b) Mazor, Y.; Steinberg, B. Z. *Phys. Rev. B* **2012**, *86*, 045120. (c) Maier, S. A.; Kik, P. G.; Atwater, H. A.; Meltzer, S.; Harel, E.; Koel, B. E.; Requicha, A. A. G. *Nat. Mater.* **2003**, *2*, 229−232. (d) Quinten, M.; Leitner, A.; Krenn, J. R.; Aussenegg, F. R. *Opt. Lett.* **1998**, *23*, 1331−1333.

(5) Neubrech, F.; Weber, D.; Katzmann, J.; Huck, C.; Toma, A.; Di Fabrizio, E.; Pucci, A.; Härtling, T. *ACS Nano* **2012**, *6*, 7326−7332.

(6) (a) Mayer, K. M.; Hafner, J. H. *Chem. Rev.* **2011**, *111*, 3828−3857. (b) Haes, A. J.; Van Duyne, R. P. *Anal. Bioanal. Chem.* **2004**, *379*, 920−930.

(7) (a) Jiang, L.; Sun, Y.; Nowak, C.; Kibrom, A.; Zou, C.; Ma, J.; Fuchs, H.; Li, S.; Chi, L.; Chen, X. *ACS Nano* **2011**, *5*, 8288−8294. (b) Duan, X.; Park, M.-H.; Zhao, Y.; Berenschot, E.; Wang, Z.; Reinhoudt, D. N.; Rotello, V. M.; Huskens, J. *ACS Nano* **2010**, *4*, 7660−7666. (c) Hicks, E. M.; Zou, S.; Schatz, G. C.; Spears, K. G.; Van Duyne, R. P.; Gunnarsson, L.; Rindzevicius, T.; Kasemo, B.; Käll, M. *Nano Lett.* **2005**, *5*, 1065−1070.

(8) (a) Guerrero-Martínez, A.; Grzelczak, M.; Liz-Marzán, L. M. *ACS Nano* **2012**, *6*, 3655−3662. (b) Liu, J.-W.; Zhang, S.-Y.; Qi, H.; Wen, W.-C.; Yu, S.-H. *Small* **2012**, *8*, 2412−2420. (c) Gao, Y.; Tang, Z. *Small* **2011**, *7*, 2133−2146. (d) Romo-Herrera, J. M.; Alvarez-Puebla, R. A.; Liz-Marzan, L. M. *Nanoscale* **2011**, *3*, 1304−1315. (e) Miszta, K.; de Graaf, J.; Bertoni, G.; Dorfs, D.; Brescia, R.; Marras, S.; Ceseracciu, L.; Cingolani, R.; van Roij, R.; Dijkstra, M.; Manna, L. *Nat. Mater.* **2011**, *10*, 872−876. (f) Prasad, B. L. V.; Sorensen, C. M.; Klabunde, K. J. *Chem. Soc. Rev.* **2008**, 37. (g) Chang, J.-Y.; Wu, H.; Chen, H.; Ling, Y.-C.; Tan, W. *Chem. Commun.* **2005**. (h) Qin, L.; Park, S.; Huang, L.; Mirkin, C. A. *Science* **2005**, *309*, 113−115.

(9) (a) Wang, L.; Xu, L.; Kuang, H.; Xu, C.; Kotov, N. A. *Acc. Chem. Res.* **2012**, 45. (b) He, J.; Liu, Y.; Babu, T.; Wei, Z.; Nie, Z. *J. Am. Chem. Soc.* **2012**, *134*, 11342−11345. (c) Liu, K.; Zhao, N.; Kumacheva, E. *Chem. Soc. Rev.* **2011**, *40*, 656−671. (d) Xu, L.; Kuang, H.; Wang, L.; Xu, C. *J. Mater. Chem.* **2011**, *21*, 16759−16782. (e) Nie, Z.; Petukhova, A.; Kumacheva, E. *Nat. Nanotechnol.* **2010**, *5*, 15−25. (f) Srivastava, S.; Kotov, N. A. *Soft Matter* **2009**, *5*, 1146−1156.

(10) De Greef, T. F. A.; Smulders, M. M. J.; Wolffs, M.; Schenning, A. P. H. J.; Sijbesma, R. P.; Meijer, E. W. *Chem. Rev.* **2009**, *109*, 5687−5754.

(11) Thomas, K. G.; Barazzouk, S.; Ipe, B. I.; Shibu Joseph, T. S.; Kamat, P. V. *J. Phys. Chem. B* **2004**, *108*, 13066−13068.

(12) Zhao, N.; Liu, K.; Greener, J.; Nie, Z.; Kumacheva, E. *Nano Lett.* **2009**, *9*, 3077−3081.

(13) Ni, W.; Mosquera, R. A.; Pérez-Juste, J.; Liz-Marzán, L. M. *J. Phys. Chem. Lett.* **2010**, *1*, 1181−1185.

(14) Chan, Y.-T.; Li, S.; Moorefield, C. N.; Wang, P.; Shreiner, C. D.; Newkome, G. R. *Chem.-Eur. J.* **2010**, *16*, 4164−4168.
(15) Nie, Z.; Fava, D.; Kumacheva, E.; Zou, S.; Walker, G. C.; Rubinstein, M. *Nat. Mater.* **2007**, *6*, 609−614.
(16) Nie, Z.; Fava, D.; Rubinstein, M.; Kumacheva, E. *J. Am. Chem. Soc.* **2008**, *130*, 3683−3689.
(17) (a) Chapel, J. P.; Berret, J. F. *Curr. Opin. Colloid Interface Sci.* **2012**, *17*, 97−105. (b) Kalsin, A. M.; Fialkowski, M.; Paszewski, M.; Smoukov, S. K.; Bishop, K. J. M.; Grzybowski, B. A. *Science* **2006**, *312*, 420−424. (c) Orendorff, C. J.; Hankins, P. L.; Murphy, C. J. *Langmuir* **2005**, *21*, 2022−2026.
(18) Li, Z.; Zhu, Z.; Liu, W.; Zhou, Y.; Han, B.; Gao, Y.; Tang, Z. *J. Am. Chem. Soc.* **2012**, *134*, 3322−3325.
(19) Taladriz-Blanco, P.; Buurma, N. J.; Rodriguez-Lorenzo, L.; Perez-Juste, J.; Liz-Marzan, L., M.; Herves, P. *J. Mater. Chem.* **2011**, *21*, 16880−16887.
(20) Fava, D.; Winnik, M. A.; Kumacheva, E. *Chem. Commun.* **2009**, *45*, 2571−2573.
(21) Liu, K.; Nie, Z.; Zhao, N.; Li, W.; Rubinstein, M.; Kumacheva, E. *Science* **2010**, *329*, 197−200.
(22) Chen, G.; Wang, Y.; Tan, L. H.; Yang, M.; Tan, L. S.; Chen, Y.; Chen, H. *J. Am. Chem. Soc.* **2009**, *131*, 4218−4219.
(23) Abbas, A.; Tian, L.; Kattumenu, R.; Halim, A.; Singamaneni, S. *Chem. Commun.* **2012**, *48*, 1677−1679.
(24) (a) Willets, K. A.; Van Duyne, R. P. *Annu. Rev. Phys. Chem.* **2007**, *58*, 267−297. (b) Yonzon, C. R.; Stuart, D. A.; Zhang, X.; McFarland, A. D.; Haynes, C. L.; Van Duyne, R. P. *Talanta* **2005**, *67*, 438−448.
(25) Stewart, M. E.; Anderton, C. R.; Thompson, L. B.; Maria, J.; Gray, S. K.; Rogers, J. A.; Nuzzo, R. G. *Chem. Rev.* **2008**, *108*, 494−521.
(26) Rycenga, M.; Cobley, C. M.; Zeng, J.; Li, W.; Moran, C. H.; Zhang, Q.; Qin, D.; Xia, Y. *Chem. Rev.* **2011**, *111*, 3669−3712.
(27) Lee, A.; Andrade, G. F. S.; Ahmed, A.; Souza, M. L.; Coombs, N.; Tumarkin, E.; Liu, K.; Gordon, R.; Brolo, A. G.; Kumacheva, E. *J. Am. Chem. Soc.* **2011**, *133*, 7563−7570.
(28) Pramod, P.; Thomas, K. G. *Adv. Mater.* **2008**, *20*, 4300.
(29) Nikoobakht, B.; El-Sayed, M. A. *Chem. Mater.* **2003**, *15*, 1957−1962.
(30) Mann, H. B.; Whitney, D. R. *Ann. Math. Stat.* **1947**, *18*, 50−60.
(31) Petukhova, A.; Greener, J.; Liu, K.; Nykypanchuk, D.; Nicolaÿ, R.; Matyjaszewski, K.; Kumacheva, E. *Small* **2012**, *8*, 731−737.
(32) Sirbiladze, K. J.; Rusznák, I.; Víg, A. *Radiat. Phys. Chem.* **2003**, *67*, 331−334.
(33) Golub, M. A.; Rosenberg, M. L. *J. Polym. Sci., Polym. Chem. Ed.* **1980**, *18*, 2543−2560.
(34) Von Raven, A.; Heusinger, H. *J. Polym. Sci., Polym. Chem. Ed.* **1974**, *12*, 2255−2271.
(35) Golub, M. A. *Macromolecules* **1969**, *2*, 550−552.
(36) Zhang, L.; Luo, Y.; Hou, Z. *J. Am. Chem. Soc.* **2005**, *127*, 14562−14563.
(37) Annunziata, L.; Duc, M.; Carpentier, J.-F. o. *Macromolecules* **2011**, *44*, 7158−7166.
(38) Slaughter, L. S.; Wu, Y.; Willingham, B. A.; Nordlander, P.; Link, S. *ACS Nano* **2010**, *4*, 4657−4666.
(39) Jain, P. K.; Eustis, S.; El-Sayed, M. A. *J. Phys. Chem. B* **2006**, *110*, 18243−18253.
(40) Odian, G. *Principles of Polymerization*, 4th ed.; Wiley: New York, 2004.
(41) Sperling, L. H. *Introduction to Physical Polymer Science*; Wiley: Hoboken, NJ, 2001.
(42) Kerle, T.; Yerushalmi-Rozen, R.; Klein, J. *Europhys. Lett.* **1997**, *38*, 207−212.
(43) Israelachvili, J. N. *Intermolecular and Surface Forces*, 3rd ed.; Academic Press: Waltham, MA, 2011.
(44) Chen, G.; Wang, Y.; Yang, M.; Xu, J.; Goh, S. J.; Pan, M.; Chen, H. *J. Am. Chem. Soc.* **2010**, *132*, 3644−3645.
(45) Fava, D.; Nie, Z.; Winnik, M. A.; Kumacheva, E. *Adv. Mater.* **2008**, *20*, 4318−4322.